HHS Public Access

Author manuscript

Curr Biol. Author manuscript; available in PMC 2017 January 25.

Published in final edited form as:

Curr Biol. 2016 January 25; 26(2): 263–269. doi:10.1016/j.cub.2015.11.064.

Motor Behavior Mediated by Continuously Generated Dopaminergic Neurons in the Zebrafish Hypothalamus Recovers After Cell Ablation

Adam D. McPherson[1], **Joshua P. Barrios**[1], **Sasha J. Luks-Morgan**[1], **John P. Manfredi**[1], **Joshua L. Bonkowsky**[2], **Adam D. Douglass**[1,3], and **Richard I. Dorsky**[1,3]

[1]Department of Neurobiology and Anatomy, University of Utah, Salt Lake City, UT

[2]Department of Pediatrics, University of Utah, Salt Lake City, Utah

Summary

Postembryonic neurogenesis has been observed in several regions of the vertebrate brain, including the dentate gyrus and rostral migratory stream in mammals, and is required for normal behavior [1–3]. Recently the hypothalamus has also been shown to undergo continuous neurogenesis as a way to mediate energy balance [4–10]. As the hypothalamus regulates multiple functional outputs, it is likely that additional behaviors may be affected by postembryonic neurogenesis in this brain structure. Here, we have identified a progenitor population in the zebrafish hypothalamus that continuously generates neurons that express *tyrosine hydroxylase* 2 (*th2*). We develop and use novel transgenic tools to characterize the lineage of *th2*+ cells and demonstrate that they are dopaminergic. Through genetic ablation and optogenetic activation we then show that *th2*+ neurons modulate the initiation of swimming behavior in zebrafish larvae. Finally we find that the generation of new *th2*+ neurons following ablation correlates with restoration of normal behavior. This work thus identifies for the first time a population of dopaminergic neurons that regulates motor behavior capable of functional recovery.

Results and Discussion

th2+ neurons are dopaminergic and arise from *dlx5/6*-expressing precursors

In the mammalian hypothalamus the embryonic neural precursor lineage expressing *Dlx* genes produces dopaminergic neurons [11]. From previous studies in our laboratory we found that neural precursors expressing a *dlx5/6* enhancer were continuously present in the

Correspondence should be addressed to A.D.D. (adam.douglass@neuro.utah.edu) or R.I.D (richard.dorsky@neuro.utah.edu). Phone: 801-581-6073 (R.I.D.); 801-587-8628 (A.D.D.).

[3]Co-senior authors

Author Contributions

All experiments were performed by A.D.M., except for *th2 in situs* (J.P.B.). S.J.L-M. and A.D.D. performed computational analysis for ChR2 experiments. Transgenic lines were made by A.D.D. [*Tg(th2:GFP-Aequorin)*^{zd201}], and by J.L.B. [*Tg(th2:Gal-VP16)*^{zd202}]. J.P.M. performed statistical analyses. A.D.D. and R.I.D. supervised all the experiments and edited the manuscript.

zebrafish hypothalamus [12]. However we failed to observe expression of Tyrosine Hydroxylase (TH), a marker of dopaminergic neurons, in this lineage using available antibodies. Because zebrafish and other non-mammalian vertebrates express a second *tyrosine hydroxylase* gene, *th2* [13, 14], we examined the expression of a transgenic reporter using 9.6 kb of *th2* upstream regulatory sequence driving *GFP-Aequorin* (Figure 1A). This construct was used to establish a stable transgenic zebrafish line [*Tg(th2:GFP-Aequorin)*^{zd201}, hereafter referred to as *th2:GFP,* Figure 1A,B], and double labeling with a *th2* mRNA probe showed extensive overlap with GFP throughout the hypothalamic posterior recess (Figure 1C). Next, we crossed the *th2:GFP* reporter line to fish expressing a *dlx5/6:mCherry* reporter, which is expressed in neural precursors [12], and analyzed coexpression in the hypothalamic posterior recess at 7 dpf. We found that 83.9% +/− 3.9% (SEM, n=5 brains) of GFP+ cells also expressed mCherry protein that persisted through terminal differentiation (Figure 1D), indicating that TH2+ neurons arise from this lineage. While a previous study concluded that *th2+* cells are serotonergic [15], we instead found that 92.8% +/− 6.9% (SEM, n=5 brains) of *th2:GFP*+ cells at 7 dpf were double labeled with a dopamine antibody (Figure 1E). In contrast, only 5.4 +/− 4.2% (SEM, n=5 brains) of *th2:GFP*+ cells were labeled with a serotonin antibody (Figure 1F). In agreement with a recent analysis using a Th2 antibody [16] we therefore conclude that *th2*+ cells are dopaminergic, and like other dopaminergic populations in mammals, are generated by *Dlx+* neural precursors.

th2+ cells are continuously generated throughout life

Because we have previously shown that hypothalamic *dlx5/6+* precursors are present through adult stages [12], we reasoned that *th2+* cells arising from these precursors might also be generated postembryonically. To test this hypothesis we administered 10 mM BrdU to *th2:GFP* transgenic larvae and adults for 24 hours, and following a chase period we found newly born GFP+ cells at 9 days post-fertilization (dpf), 25 dpf, and 6 months post-fertilization (mpf) (Figure 2A–C). Consistent with a higher rate of neurogenesis in younger animals, the BrdU labeling index was 10.4% with only 3 days of chase in early larvae (9 dpf), 5.9% with 2 weeks of chase in late larvae (25 dpf), and 1.1% with 2 weeks of chase in adults (Figure 2D). We observed a higher BrdU labeling index in the *dlx5/6*+ precursor population at all stages (data not shown), suggesting that the birth of *th2*+ neurons may be more tightly regulated, perhaps in response to environmental signals. Overall, our data indicate that along with other cell types [12], zebrafish constantly generate dopaminergic neurons in the hypothalamus into adulthood.

Ablation of *th2*+ neurons reduces swimming frequency

While a function for hypothalamic *th2+* neurons in the modulation of motor function has been previously suggested [17], a definitive behavioral analysis of this population has not been performed due to the lack of specific genetic tools. We therefore took a genetic approach to ablate *th2*+ cells and examine the resulting effects on behavior. We generated a *th2:Gal4* transgenic line [*Tg(th2:Gal-VP16)*^{zd202}] which was crossed to *Tg(UAS-E1b:NTR-mCherry)*^{c264} fish [18] to drive Nitroreductase (NTR) expression in *th2*+ neurons (Figure S1A) and enable chemical ablation [19, 20]. While the hypothalamic posterior recess of untreated brains had an average of 128.7 ± 20.6 mCherry+ cells (S.E.M., n=7 brains), after

addition of 5 mM metronidazole (MTZ) to double transgenic embryos from 5–7 dpf, we observed a reduction to 18.1 ± 2.4 cells/brain (S.E.M., n=10 brains), a decrease of 86% (Figure 3A–B). The effects of ablation on spontaneous swimming were then measured in single 8 dpf larvae over a ten-minute recording period, during which the animals were allowed to move freely within a dish. Ablation of *th2+* neurons significantly reduced both the bout frequency and total amount of time spent swimming, but not the amplitude of individual swimming bouts (Figure 3C–E, Figure S1C, Movies S1–S2, p=0.009 for swim frequency; p=0.020 for swim time by 2-way ANOVA). In contrast treating non-transgenic siblings with MTZ (Figure 3C–E), and ablation of hypothalamic radial glia using a separate transgenic line [18] (Figure S1D–E), did not affect swimming behavior. Decreased frequency of swimming was also observed following MTZ treatment of an independent transgenic line, expressing NTR-GFP directly under the control of the *th2* enhancer (Figure 3F–I and Figure S1B). Our data thus suggest that *th2*+ neurons regulate the initiation of movement.

Activation of *th2*+ neurons increases swim frequency

To test the sufficiency of *th2+* neurons for the initiation of swimming, we expressed Channelrhodopsin-2 (ChR2) in these cells by crossing *Tg(UAS:ChR2-YFP)*^{u144} [21] and *Tg(th2:Gal-VP16)*^{zd202} fish (Figure S1E) Expression of the ChR2-YFP fusion protein specifically in posterior recess neurons allowed us to examine their axon trajectory and targets using whole-brain confocal imaging (Figure 3J; Movie S3). We found that a majority of axons appear to terminate a short distance from the posterior recess, likely in the posterior tuberculum. This projection pattern differentiates the *th2*+ neurons from *th1*− expressing cells in the posterior recess, which primarily innervate local hypothalamic targets [22].

Freely moving larvae in a dish were then stimulated with 5-second pulses of blue light delivered once per minute over a 10-minute period, causing activation of the cells as indicated by *cfos* expression (Figure S1G). During the blue light pulse, larvae from ChR2+ crosses showed increased frequency of swimming compared to controls (Figure 3K, Figure S1H, Movies S4–5). Automated tracking revealed that increased bout frequency during the stimulus resulted in a significant increase in the animal's cumulative displacement compared to baseline (Figure S1I–J). Together with the ablation experiments, these data indicate that *th2*+ neurons may function either in the direct activation of motor behavior, or as suggested previously, in modulating the threshold of a motor response to sensory-evoked stimuli [17].

th2+ neurons are restored after ablation

Based on our observations that *th2*+ neurons are continuously generated like other cells in the zebrafish hypothalamus [12], we hypothesized that this cell population may have the ability to recover following ablation. We therefore performed ablations from 5–7 dpf and behavioral analysis at 8 dpf as described above, then treated the same larvae with 10 mM BrdU for two days (8–10 dpf), and allowed them to recover for 2 weeks before receiving an acute treatment of 5 mM MTZ or 0.5% DMSO. Following immunohistochemistry with mCherry and BrdU antibodies, ablated animals showed a striking recovery in the overall mCherry+ population (Figure 4A,B,E). While these data do not allow us to distinguish true regeneration from the normal process of cell addition during the experiment, we observed a

significant increase in the fraction of newly born mCherry+ cells compared to unablated controls, consistent with a regenerative response (Figure 4F). The actual level of neurogenesis was likely even higher, due to the fact that progenitors becoming postmitotic before 8 dpf were not labeled with BrdU. In a separate study, we have also observed a transient increase in BrdU uptake by neural progenitors 2 days after ablation of *th2+* neurons [23]. Together, these data show that *th2+* neurons are capable of recovery after injury, similar to dopaminergic neurons in the mammalian olfactory bulb [24]. Interestingly, those neurons arise from progenitors expressing a similar series of developmental transcription factors as we have observed in the zebrafish hypothalamus [12, 25].

Replacement of *th2* neurons correlates with recovery of swimming deficits

Because adult-born *th2+* cells extend both short radial processes into the ventricle and long projections (Figure 2C), we hypothesized that cells born after ablation may be capable of re-integrating into existing circuits. We therefore tested whether *th2*+ cell replacement led to functional recovery of the swimming deficits resulting from their ablation. Following a two-week recovery period, MTZ-treated and control fish received another treatment with MTZ or DMSO (Figure 4A–E), and behavioral analysis was performed on groups of 3 larvae. Fish in which the *th2*+ neurons had been ablated at 7 dpf displayed swimming behavior indistinguishable from that of unablated siblings ($p=0.60$ for swim frequency; $p=0.80$ for swim time by 2-way ANOVA), while fish receiving an ablation at 25 dpf displayed a significant decrease in swimming bout frequency and time spent swimming (Figure 4G–H, Figure S2, $p=0.034$ for swim frequency; $p=0.032$ for swim time by 2-way ANOVA). While *th2+* neurons are likely only one of many cell types in the zebrafish brain that can be restored after ablation, our data indicate a strong correlation between the replacement of *th2*+ cells and functional recovery of the behavior they regulate. Proof of functional integration into circuitry will require further analysis of physiological activity, but our results are consistent with this possibility.

Conclusions

This study provides the first genetic analysis of the *th2+* neuronal population in the zebrafish hypothalamus. We have shown that *th2*+ neurons are dopaminergic and arise from *dlx5/6*+ precursors, similar to dopaminergic neurons in the mammalian hypothalamus and olfactory bulb. In addition, we find that *th2*+ neurons regulate the frequency of spontaneous swimming, providing the first genetically validated link between these neurons and a behavioral function. Most intriguingly, our data indicate *th2*+ neurons are replaced within 2 weeks after ablation, coinciding with a recovery of normal swimming behavior. Together, our findings suggest that even in non-regenerative mammalian systems, replacement of dopaminergic neurons that modulate motor function after loss from disease or injury could potentially support the recovery of normal behavior.

Experimental Procedures

Use of zebrafish

Larvae were raised in E3 medium at 28.5°C until 5–7 dpf at which point they were fed daily until analysis. Larval and adult brains were obtained by dissection from animals fixed in 4% paraformaldehyde + 5% sucrose in PBS. Ablations were performed by immersion in E3 media containing 5 mM MTZ in 0.5% DMSO for 2 days in the dark. BrdU labeling of larvae was performed by immersion in E3 medium with 10 mM BrdU in the dark. Adult fish were injected interperitoneally with 10 mM BrdU in 110 mM NaCl. All procedures were approved by the IACUC committee at the University of Utah.

Generation of transgenic lines

For *th2:GFP-Aequorin, th2:Gal4-VP16,* and *th2:ChR2-tRFP* transgenes, a 9.6 kb regulatory sequence flanking the 5' end of the *th2* open reading frame was cloned by gap repair recombineering (http://ncifrederick.cancer.gov/research/brb/recombineeringInformation.aspx) from BAC clone CH211-260P3 into a Gateway donor vector to make *pENTR:th2(9.6kb)*. This vector was used for LR cloning into destination vectors containing *GFP-Aequorin, Gal4-VP16*, or *ChR2-tRFP* coding sequence flanked by Tol2 transposon sites. The *th2:NTR-EGFP* transgene was generated by replacement of the *ChR2-tRFP* coding sequence with an *NTR-eGFP* coding sequence [25] in the destination vector using restriction digestion and ligation.

To generate stable transgenic lines for *th2:GFP-Aequorin* and, *th2:Gal4-VP16*, 10–50 pg of DNA was injected into fertilized, single-cell zebrafish embryos along with 20–30 pg Tol2 mRNA to enable genomic integration. Founder animals were identified by outcrossing and screening progeny for fluorescence, or by PCR detection of the transgene. Individual lines were established after two successive generations of outcrossing to WT animals. Allele designations for stable lines are *Tg(th2:GFP-Aequorin)*^{zd201} and *Tg(th2:Gal-VP16)*^{zd202}.

In situ hybridization and immunohistochemistry

In situ hybridization was performed as previously described in [27]. Antisense probe for *th2* was generated by PCR amplification using the primers below, followed by transcription with T7 RNA Polymerase. *th2* primers: 5'- CGGAGACAGCTTCGTGTT, 3'-GCTCATTAGAAAGGGCATA. *cfos* probe was made as previously described [28]

Immunohistochemistry was performed as previously described in [18], with the addition of treatment with 2 N HCl for 30–60 minutes for BrdU detection.

The following primary antibodies were used: Rabbit anti-DA (purchased from H.W.M. Steinbusch), Rabbit anti-5HT (Sigma, S5545), Mouse anti-GFP (Invitrogen, A11120), Rabbit anti-GFP (Invitrogen, A11122), Chicken anti-GFP (Aves, GFP-1020), Rabbit anti-dsRed (Clontech, 632496), Mouse anti-BrdU (DSHB, G3G4-BrdU), Chicken anti-BrdU (Aves, CBDU-65A-Z)

The following secondary antibodies were used: Goat anti-Mouse Alexa Fluor 448 (Invitrogen, A11001), Goat anti-Rabbit Alexa Fluor 488 (Invitrogen, A11008), Donkey anti-

Chicken Alexa Fluor 488 (Jackson ImmunoResearch, 703-545-155), Goat anti-Chicken Alexa Fluor 568 (Invitrogen, A11041), Goat anti-Mouse Alexa Fluor 633 (Invitrogen, A21050), Goat anti-Chicken Alexa Fluor 633 (Invitrogen, A21103), Goat anti-Mouse Alexa Fluor 647 (Invitrogen, A21235), Goat anti-Rabbit Alexa Fluor 647 ((Invitrogen, A21244), Goat anti-Chicken Alexa Fluor 647 (Invitrogen, A21449)

Microscopy

Whole larval brains were imaged ventrally through the entire hypothalamus, determined by the anatomy of the 3rd ventricle and posterior recess. Adult brains were bisected midsagittally and imaged laterally from the midsagittal surface. Images were collected on an Olympus FV1000 confocal microscope, an Olympus BX51WI compound fluorescence microscope, and an Olympus SZX16 fluorescence dissecting microscope. Image quantification was performed with ImageJ software, and images were processed for figures using Adobe Photoshop.

Behavior

All behavioral measurements were made on a custom-built apparatus in which the movements of free-swimming animals were monitored using a Pike CCD camera (Allied Vision Tech, Stadtroda, Germany) controlled by custom LabView software (National Instruments, Austin, TX). For optogenetics experiments, animals were stimulated with 470 nm light from a high-power LED at 0.6 mW/mm^2, distributed uniformly across the arena with a condenser lens and photographic diffuser paper. Movement was analyzed online using a running frame subtraction, in which the maximal pixel intensity change in each difference image was computed and then saved. Frames in which the fish moved were apparent as transient spikes in this vector. Subsequent analysis in MATLAB identified swim bouts using a spike-finding algorithm and computed the amplitude and frequency of these events as a measure of locomotor activity. Automated tracking analyses were performed by applying custom MATLAB scripts to movies of the behavior acquired at 404 frames/s, then measuring each animal's instantaneous velocities and cumulative displacement during the stimulus and baseline periods.

Statistical analyses

Single variable pairwise comparisons were analyzed using a Student t-test. Multivariable datasets were analyzed using ANOVA, followed by Bonferroni Multiple Comparisons test to produce multiplicity-adjusted p values for pairwise comparisons. Significance was defined as a p value of 0.05 or smaller. Outliers were excluded at $p<0.01$, using Grubbs' test.

Supplementary Material

Refer to Web version on PubMed Central for supplementary material.

Acknowledgements

We thank the University of Utah Centralized Zebrafish Animal Resource (CZAR) for assistance with animal care and the Cell Imaging Core for assistance with confocal microscopy. We thank Shiela Samson for making the *th2 in situ* probe, and Janet Iwasa for assistance with the graphical abstract.

A.D.D. was funded by a Sloan Foundation Research Fellowship, R.I.D was funded by NIH R01 NS082645, and. J.L.B. was funded by NIH DP2 MH100008. A.D.M. was funded by NIH 5T32 HD07491 and A.D.M. and S.J.L.-M. were both funded by NIDCD 5T32 DC008553.

References

1. Gould E. How widespread is adult neurogenesis in mammals? Nature reviews. Neuroscience. 2007; 8:481–488.
2. Aimone JB, Li Y, Lee SW, Clemenson GD, Deng W, Gage FH. Regulation and function of adult neurogenesis: from genes to cognition. Physiological Reviews. 2014; 94:991–1026. [PubMed: 25287858]
3. Imayoshi I, Sakamoto M, Ohtsuka T, Takao K, Miyakawa T, Yamaguchi M, Mori K, Ikeda T, Itohara S, Kageyama R. Roles of continuous neurogenesis in the structural and functional integrity of the adult forebrain. Nature Neuroscience. 2008; 11:1153–1161. [PubMed: 18758458]
4. Bolborea M, Dale N. Hypothalamic tanycytes: potential roles in the control of feeding and energy balance. Trends in Neurosciences. 2013; 36:91–100. [PubMed: 23332797]
5. Maia V, Kokoeva HY, Jeffrey S, Flier. Neurogenesis in the Hypothalamus of Adult Mice: Potential Role in Energy Balance. Science. 2005; 310:679–683. [PubMed: 16254185]
6. Pierce AA, Xu AW. De novo neurogenesis in adult hypothalamus as a compensatory mechanism to regulate energy balance. The Journal of Neuroscience. 2010; 30:723–730. [PubMed: 20071537]
7. Li J, Tang Y, Cai D. IKKbeta/NF-kappaB disrupts adult hypothalamic neural stem cells to mediate a neurodegenerative mechanism of dietary obesity and pre-diabetes. Nature Cell Biology. 2012; 14:999–1012. [PubMed: 22940906]
8. Lee DA, Blackshaw S. Functional implications of hypothalamic neurogenesis in the adult mammalian brain. International Journal of Developmental Neuroscience. 2012; 30:615–621. [PubMed: 22867732]
9. Cheng MF. Hypothalamic neurogenesis in the adult brain. Frontiers in Neuroendocrinology. 2013; 34:167–178. [PubMed: 23684668]
10. Sousa-Ferreira L, de Almeida LP, Cavadas C. Role of hypothalamic neurogenesis in feeding regulation. Trends in Endocrinology and Metabolism. 2014; 25:80–88. [PubMed: 24231724]
11. Yee CL, Wang Y, Anderson S, Ekker M, Rubenstein JL. Arcuate nucleus expression of NKX2.1 and DLX and lineages expressing these transcription factors in neuropeptide Y(+), proopiomelanocortin(+), and tyrosine hydroxylase(+) neurons in neonatal and adult mice. The Journal of Comparative Neurology. 2009; 517:37–50. [PubMed: 19711380]
12. Wang X, Kopinke D, Lin J, McPherson AD, Duncan RN, Otsuna H, Moro E, Hoshijima K, Grunwald DJ, Argenton F, et al. Wnt signaling regulates postembryonic hypothalamic progenitor differentiation. Developmental Cell. 2012; 23:624–636. [PubMed: 22975330]
13. Yamamoto K, Ruuskanen JO, Wullimann MF, Vernier P. Differential expression of dopaminergic cell markers in the adult zebrafish forebrain. The Journal of Comparative Neurology. 2011; 519:576–598. [PubMed: 21192085]
14. Yamamoto K, Ruuskanen JO, Wullimann MF, Vernier P. Two tyrosine hydroxylase genes in vertebrates: New dopaminergic territories revealed in the zebrafish brain. Molecular and Cellular Neurosciences. 2010; 43:394–402. [PubMed: 20123022]
15. Ren G, Li S, Zhong H, Lin S. Zebrafish tyrosine hydroxylase 2 gene encodes tryptophan hydroxylase. The Journal of Biological Chemistry. 2013; 288:22451–22459. [PubMed: 23754283]
16. Semenova SAC, Y C, Zhao X, Rauvala H, Panula P. The tyrosine hydroxylase 2 (TH2) system in zebrafish brain and stress activation of hypothalamic cells. Histochem. Cell Biol. 2014; 142:619–633. [PubMed: 25028341]
17. Mu Y, Li XQ, Zhang B, Du JL. Visual input modulates audiomotor function via hypothalamic dopaminergic neurons through a cooperative mechanism. Neuron. 2012; 75:688–699. [PubMed: 22920259]
18. Otsuna H, Hutcheson D, Duncan R, McPherson A, Scoresby A, Gaynes B, Tong Z, Fujimoto E, Kwan K, Chien C, et al. High-resolution analysis of CNS expression patterns in zebrafish Gal4 enhancer-trap lines. Developmental Dynamics. 2015; 244:785–796. [PubMed: 25694140]

19. Curado S, Anderson RM, Jungblut B, Mumm J, Schroeter E, Stainier DY. Conditional targeted cell ablation in zebrafish: a new tool for regeneration studies. Developmental Dynamics. 2007; 236:1025–1035. [PubMed: 17326133]
20. Curado S, Stainier DY, Anderson RM. Nitroreductase-mediated cell/tissue ablation in zebrafish: a spatially and temporally controlled ablation method with applications in developmental and regeneration studies. Nature Protocols. 2008; 3:948–954. [PubMed: 18536643]
21. Lacoste AM, Schoppik D, Robson DN, Haesemeyer M, Portugues R, Li JM, Randlett O, Wee CL, Engert F, Schier AF. A convergent and essential interneuron pathway for Mauthner-cell-mediated escapes. Current Biology. 2015; 25:1526–1534. [PubMed: 25959971]
22. Tay TL, Ronneberger O, Ryu S, Nitschke R, Driever W. Comprehensive catecholaminergic projectome analysis reveals single-neuron integration of zebrafish ascending and descending dopaminergic systems. Nature Communications. 2011; 2:171.
23. Duncan RN, Xie Y, McPherson AD, Taibi AV, Bonkowsky JL, Douglass AD, Dorsky RI. Hypothalamic radial glia function as self-renewing neural progenitors in the absence of Wnt/β-catenin signaling. Development. 2015 *in press*.
24. Schwob JE. Neural regeneration and the peripheral olfactory system. The Anatomical Record. 2002; 269:33–49. [PubMed: 11891623]
25. Lee JE, Wu SF, Goering LM, Dorsky RI. Canonical Wnt signaling through Lef1 is required for hypothalamic neurogenesis. Development. 2006; 133:4451–4461. [PubMed: 17050627]
26. Lambert AM, Bonkowsky JL, Masino MA. The conserved dopaminergic diencephalospinal tract mediates vertebrate locomotor development in zebrafish larvae. The Journal of Neuroscience. 2012; 32:13488–13500. [PubMed: 23015438]
27. Thisse C, Thisse B. High-resolution in situ hybridization to whole-mount zebrafish embryos. Nature Protocols. 2008; 3:59–69. [PubMed: 18193022]
28. von Trotha JW, Vernier P, Bally-Cuif L. Emotions and motivated behavior converge on an amygdala-like structure in the zebrafish. The European Journal of Neuroscience. 2014; 40:3302–3315. [PubMed: 25145867]

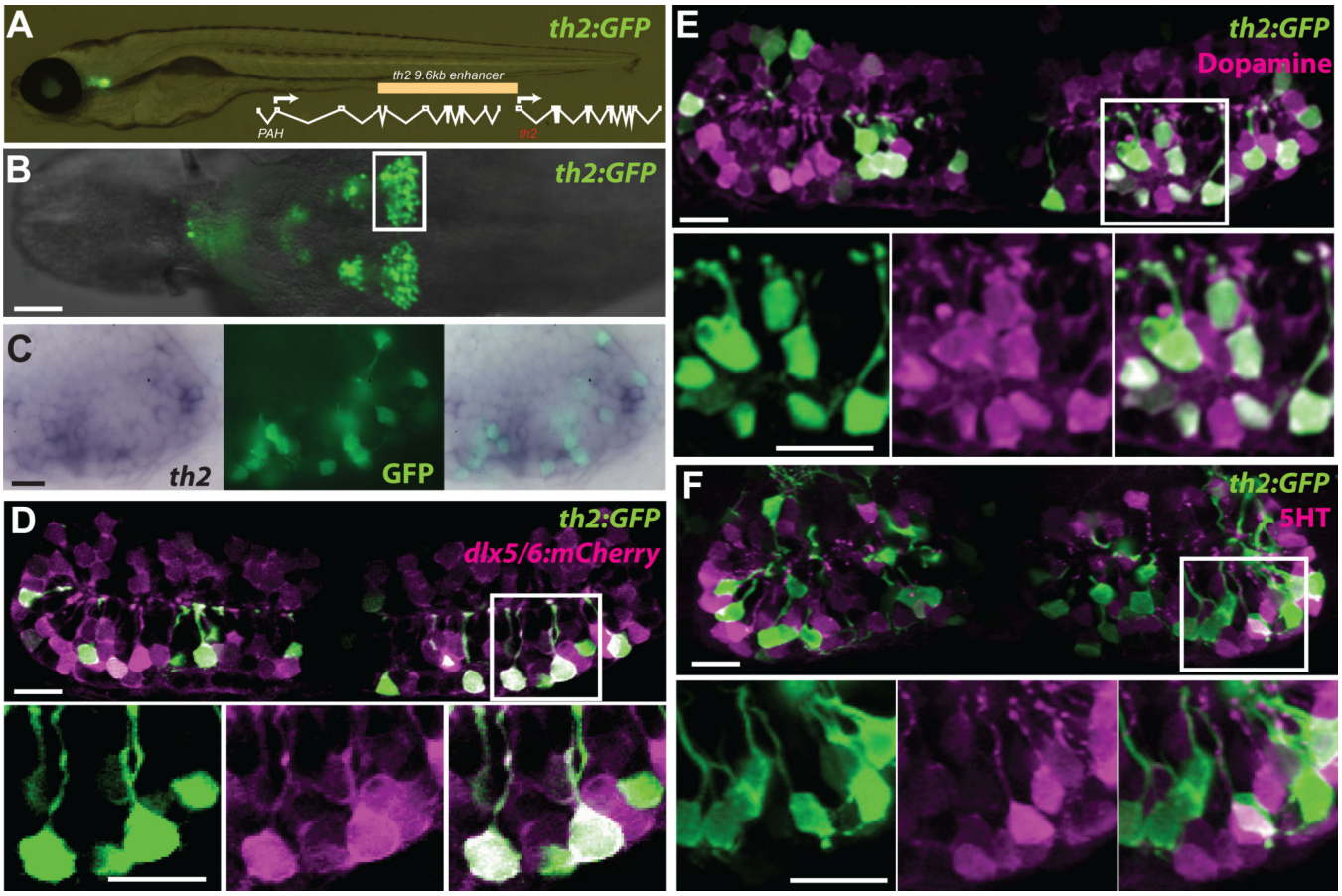

Figure 1. A *th2:GFP* transgene labels dopaminergic neurons derived from a *dlx5/6+* precursor lineage

(A) Live zebrafish 7 dpf larva expressing *th2:GFP* with schematic of *th2* enhancer/promoter region used for transgenes. (B) Ventral whole-mount view of *th2:GFP* expression in a dissected 7 dpf brain, box indicates area of posterior recess shown in (C–F). (C) Simultaneous *in situ* hybridization for *th2* mRNA (left) and anti-GFP immunohistochemistry (middle) shows transcript expression in all *th2:GFP+* cells (right). Ventral whole-mount view of a dissected 7 dpf brain is shown. (D) Co-expression analysis shows that most *th2:GFP+* cells (green) express *dlx5/6:mCherry* (magenta), indicating their origin from *dlx5/6+* precursors. (E) Co-expression analysis shows that most *th2:GFP+* cells (green) express dopamine (magenta). (F) Co-expression analysis shows that few *th2:GFP+* cells (green) express serotonin (magenta). All images in (D–F) are ventral maximum intensity confocal Z-projections of the hypothalamic posterior recess from dissected 7 dpf brains. Individual and merged channels of boxed regions are shown in lower panels. Scale bar in (B) = 50μm, all other scale bars = 10μM.

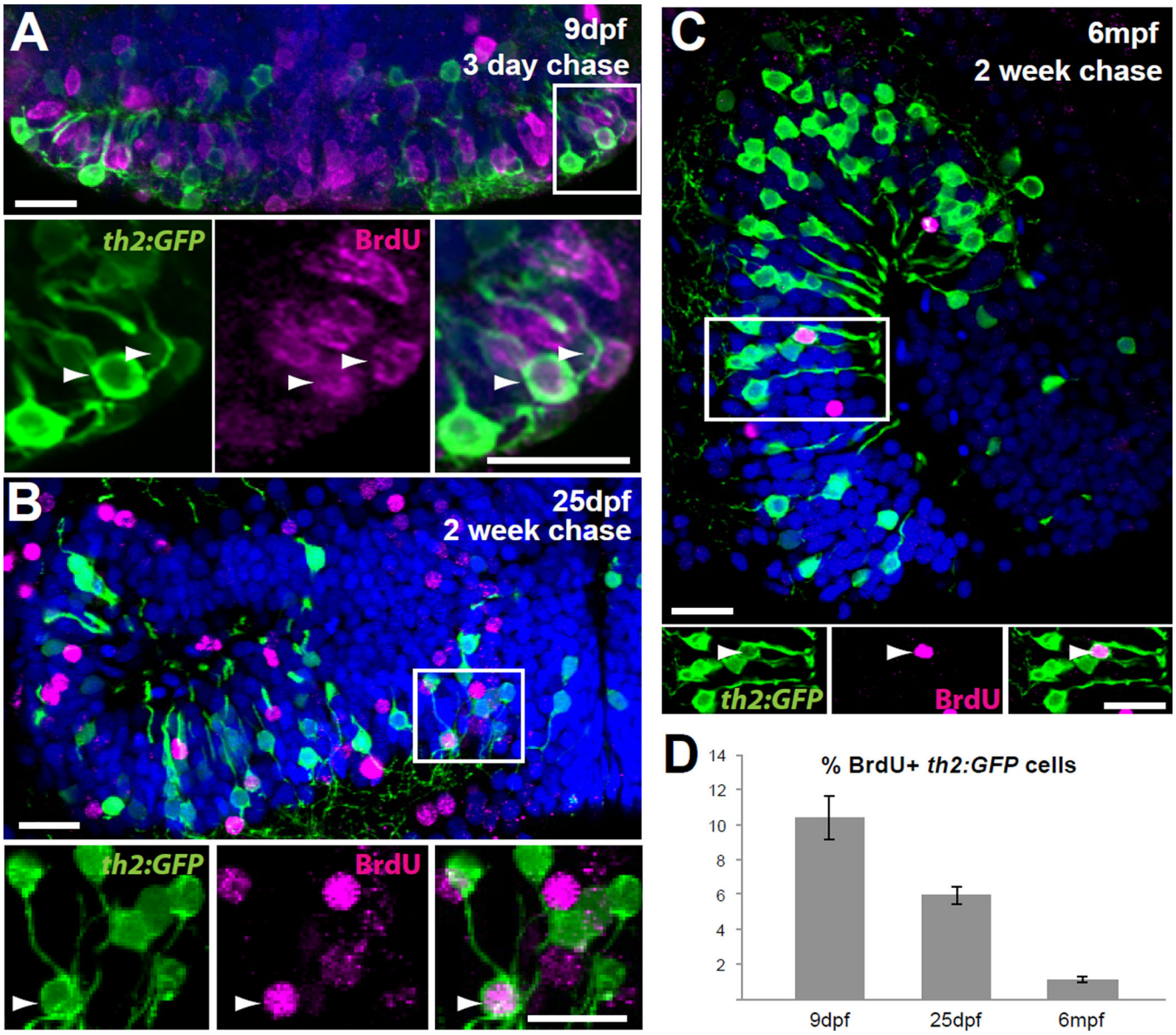

Figure 2. *th2* + cells are continuously generated throughout life

(A) 5 dpf larvae were treated with BrdU for 24 hours and analyzed at 9 dpf. Numerous *th2:GFP+* cells (green) are labeled with BrdU (magenta) in the hypothalamic posterior recess. Arrowheads indicate double-labeled cells. (B) 12 dpf larvae were treated with BrdU for 24 hours and analyzed at 25 dpf. *th2:GFP+* cells (green) labeled with BrdU (magenta) can be found in medial regions of the hypothalamic posterior recess. Arrowheads indicate double-labeled cells. (C) 6 mpf fish were injected interperitoneally with BrdU and analyzed 2 weeks later. *th2:GFP+* cells (green) labeled with BrdU (magenta) can be found in a midsagittal view of the hypothalamic posterior recess. Arrowheads indicate double-labeled cells. (D) Percent of BrdU+ cells in the *th2:GFP*+ population throughout the entire posterior recess. Error bars=SEM, n=5 brains. Images in (A–B) are ventral maximum intensity confocal Z-projections of the hypothalamic posterior recess. Images in (C) are maximum intensity confocal Z-projections from midsagittal views of the hypothalamic posterior

recess. Individual and merged channels of boxed region are shown in lower panels. Scale bars=10μM.

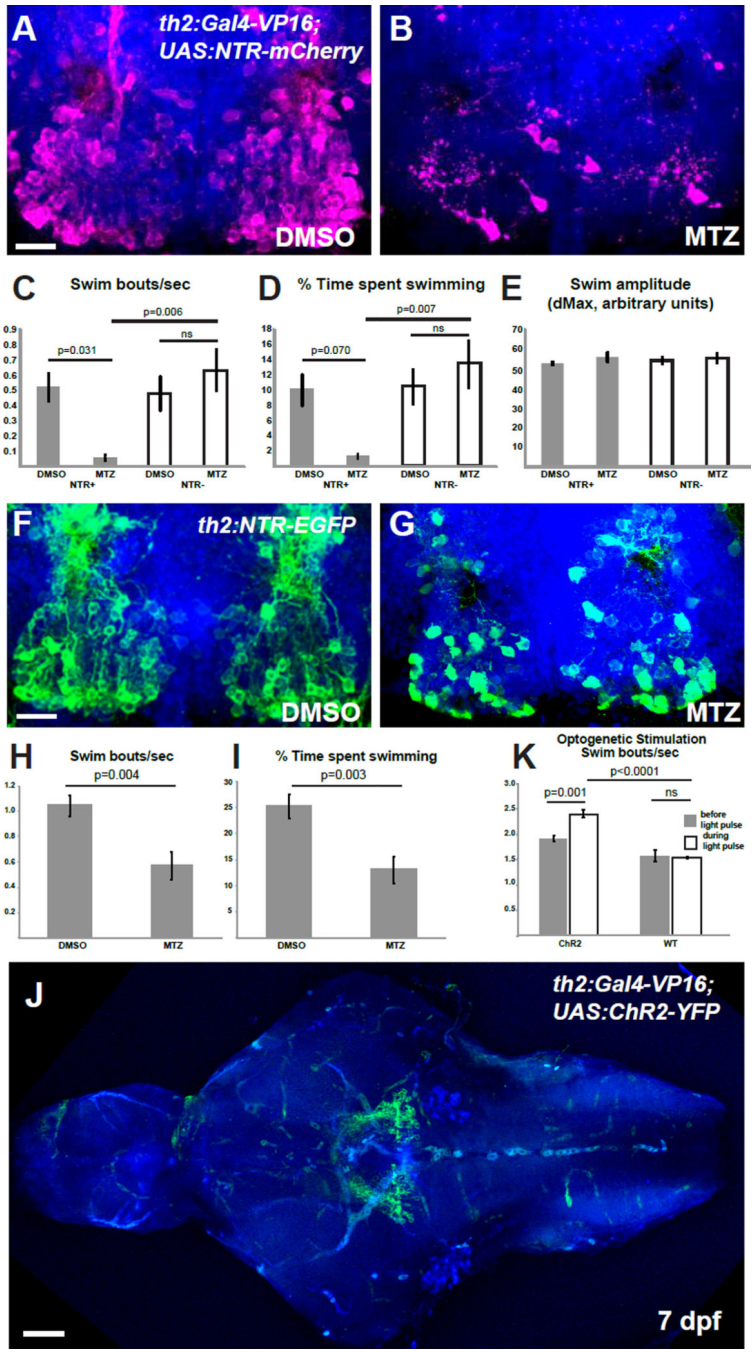

Figure 3. *th2*+ cells modulate the initiation of swimming behavior

(A–B) Representative brains of 8 dpf *th2:Gal4-VP16; UAS:NTR-mCherry* larvae treated with 0.5% DMSO (A) or 5mM MTZ (B) from 5–7 dpf. (C–E) Effects of ablation on behavior in 8 dpf larvae as measured by swimming frequency (C) time spent swimming (D), and swim amplitude (E) Error bars=SEM, n=6 larvae for each condition except NTR+ fish treated with MTZ, wherein n=5 due to exclusion of an outlier ($p<0.01$, Grubbs' test). Two-way ANOVA indicates a significant interaction between genotype and treatment for swim initiations ($p=0.009$ for swim frequency; $p=0.020$ for swim time), but not for swim

amplitude. Adjusted p values shown for pairwise comparisons are based on Bonferroni Multiple Comparison test. (F–G) Representative brains from 8 dpf *th2:NTR-EGFP* larvae treated with 0.5% DMSO (F) or 5mM MTZ (G) from 5–7 dpf. (G–H) Effects of ablation on swimming behavior in 8 dpf larvae as measured by swimming frequency (H) and time spent swimming (I). Error bars=SEM, n=8 individual larvae for each condition. p values based on Student t-test. See Figure S1 for whole-animal images of NTR transgene expression, representative plots of swimming behavior, and control ablations of radial glia. (J) Representative brain of *th2:Gal4: UAS:ChR2-YFP* larva, showing that most axons appear to terminate nearby in the posterior tuberculum. (K) Average swim bouts/sec before and during blue light pulse for individual larvae. Error bars=SEM, n=4 (wild-type), n=5 (ChR2). Two-way ANOVA demonstrates significant interaction between genotype and light exposure (p=0.0025). Adjusted p values shown for pairwise comparisons are based on Bonferroni Multiple Comparison test. Images in (A–B,F–G,J) are ventral maximum intensity confocal Z-projections of the brain. Scale bar = 10μM. See Figure S1 for whole-animal images of ChR2 expression, and examples of neuronal activity and swimming behavior after stimulation.

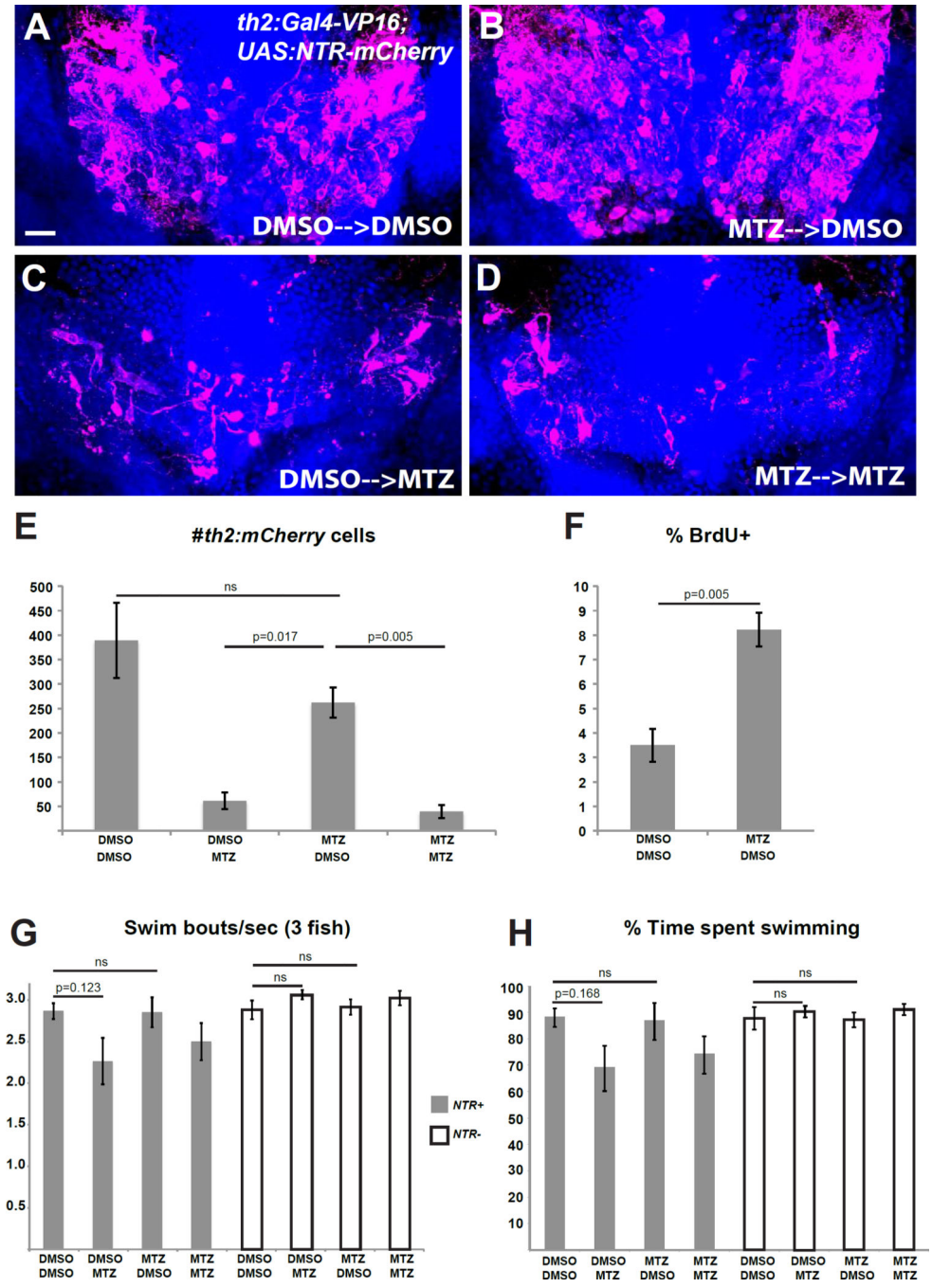

Figure 4. *th2*+ cells are replaced after ablation and mediate functional recovery of swimming behavior

(A–D) Representative brains from *th2:Gal4-VP16; UAS:NTR-mCherry* larvae that were treated with 0.5% DMSO or 5mM MTZ from 5–7 dpf, followed by 10 mM BrdU from 8–10 dpf and allowed to recover for two weeks (10–25 dpf) before acute treatments with 0.5% DMSO or 5mM MTZ. (E) Recovery of *th2*+ cells measured by total cell number. Analysis of the 4 groups by 2-way ANOVA indicates that the 25 dpf treatment has a significant effect on the number of *th2:mCherry* cells at 28 dpf (p=0.0001), while the 7 dpf treatment does not (p=0.082); nor is there a significant interaction between two successive treatments (p=0.20).

Adjusted p values shown for pairwise comparisons are based on Bonferroni Multiple Comparison test. n=3 brains for larvae untreated at 7 dpf, n=4 brains for larvae treated with MTZ at 7 dpf. (F) Percent labeled by BrdU at 8 dpf. Error bars=SEM, n=5 brains. p value based on Student t-test. (G–H) Recovery of behavior 3 weeks after ablation as measured by swimming frequency (G) and time spent swimming (H), n=5 groups for each condition except n=4 for wild-type larvae treated with MTZ+DMSO after exclusion of an outlier ($p<0.001$, Grubbs' test). Statistical analyses were performed separately for the wild-type and NTR+ larvae. Two-way ANOVA of wild-type larvae shows no significant effect of either the 7 dpf treatment ($p=0.95$ for swim frequency; $p=0.89$ for swim time) or the 25 dpf treatment ($p=0.13$ for swim frequency; $p=0.37$ for swim time) at 28 dpf, and there is no significant interaction between the successive treatments ($p=0.66$ for swim frequency; $p=0.76$ for swim time). For NTR+ larvae, 2-way ANOVA indicates that the 7 dpf treatment does not affect swimming behavior at 28 dpf ($p=0.60$ for swim frequency; $p=0.80$ for swim time), while the 25 dpf treatment has a significant effect ($p=0.034$ for swim frequency; $p=0.032$ for swim time). There was no significant interaction between the successive treatments ($p=0.55$ for swim frequency; $p=0.64$ for swim time). Adjusted p values shown for pairwise comparisons are based on Bonferroni Multiple Comparison test. Images in (A–D) are ventral maximum intensity confocal Z-projections of the hypothalamic posterior recess. Scale bar = 10μM. See Figure S2 for representative plots of swimming behavior in ablated and unablated animals.